PHYSICAL REVIEW B VOLUME 34, NUMBER 8 15 OCTOBER 1986

Properties of the $EL2$ level in $GaAs_{1-x}P_x$

L. Samuelson and P. Omling
Department of Solid State Physics, University of Lund, Box 118, S-221 00 Lund, Sweden

(Received 1 April 1986)

In this paper the properties of the $EL2$ level are studied as a function of the composition x in the alloy system $GaAs_{1-x}P_x$. From photoionization cross sections and thermal emission data the ground state of the $EL2$ level can be followed through the alloy system with respect to energy position, spectral details in optical cross sections, and thermal emission rates giving information on how the ground and excited states vary relative to the band structure in the alloy. Comparing our data extended to GaP with published properties of GaP defects we strongly reduce the number of candidates for an $EL2$-related defect in GaP, and tentatively suggest a candidate for a defect in GaP corresponding to $EL2$. The limited composition range in which the metastable state of $EL2$ has been observed is found to coincide with compositions for which the excited $EL2$ state is degenerate in energy with the conduction band.

I. INTRODUCTION

An important and thoroughly investigated defect in GaAs is the midgap donor level $EL2$, which has been found to be the dominant electron trap in both bulk-grown and vapor-phase-epitaxially grown materials.[1] This level plays an important role in the compensation mechanism leading to semi-insulating GaAs. In spite of a large amount of experimental data, neither detailed properties nor the microscopic identity of this defect have been established. Historically this level has also been labeled the "O" level since it was originally attributed to oxygen. This assignment was partly due to a correlation with the presence of oxygen during the material preparation and partly due to a missing oxygen-related deep level in GaAs.[1,2] This missing level is in contrast to the case of GaP where oxygen is known to occupy a phosphorous lattice site substitutionally, thereby generating the 0.9-eV deep donor level.[3] Later a direct correlation between $EL2$ and oxygen in GaAs has generally been regarded as disputable.[1] Instead, several experimental results have shown that the formation of $EL2$ is determined by the stoichiometric condition during growth, thereby suggesting the involvement of native defects.[4–6] Since it was shown by EPR that defects involving As_{Ga} are present in $EL2$-containing material, anion antisite defects have been discussed as possible candidates for the $EL2$ level.[7,8] However, it has been found that this hypothesis is very difficult to test.

In an attempt to trace the $EL2$ level from GaAs to GaP, we have previously reported properties of the excited states (branching state $EL2^e$ and metastable state $EL2^*$) in the $GaAs_{1-x}P_x$ alloy system.[9] In this work, we have established the ground-state properties ($EL2^g$) of the level in the alloy system by measuring the thermal and optical properties of the defect. The importance of this is twofold. First, we are able to extrapolate the energy position of the $EL2$ level through the alloy system to GaP. Second, by combining the result for the ground-state position with that for the position of the excited state $EL2^e$, and plotting these in the $GaAs_{1-x}P_x$ band diagram, we obtain "boundary conditions" that should be satisfied by an appropriate model for the $EL2$ defect.

II. EXPERIMENTAL DETAILS

The material used in this work was grown by (metal-organic vapor-phase epitaxy (MOVPE). Using the results from a previous investigation of the thermodynamical conditions for the formation of the $EL2$ level in GaAs,[4] it has been possible to obtain "tailor-made" $GaAs_{1-x}P_x$ material with $EL2$ concentrations which allows investigations of the defect by space-charge techniques. Details of the epitaxial growth and the material properties have been published elsewhere.[10,11]

All measurements presented here have been performed on Schottky diodes produced by Cr evaporation on nonintentionally doped n-type $GaAs_{1-x}P_x$. The carrier concentrations, determined by $1/C^2$-V measurements, varied between 5×10^{15} and 3×10^{16} cm^{-3}, with the high values being observed for P-rich materials. The composition of each diode is determined with an accuracy of $\pm0.5\%$ by microprobe analysis using characteristic x-ray emission. Deep-level transient spectroscopy (DLTS) has been used to measure thermal emission rates, thermal activation energies, alloy-broadening parameters, and deep-level concentrations.[12,13] Photoionization cross sections have been obtained from the analysis of time constants in photocapacitance measurements.[14]

III. EXPERIMENTAL RESULTS AND DISCUSSION

A. Identification of $EL2$ in the $GaAs_{1-x}P_x$ alloy

Due to its specific properties, the $EL2$ level in GaAs is readily identified. The thermal emission rate, e_n^t, as a function of inverse temperature is one of the properties specific to $EL2$, even though care must be taken since at least two types of defects with almost identical thermal emission rates can occur depending on the type of material investigated.[15,16] In Fig. 1, e_n^t/T^2 is plotted versus $1/T$ for GaAs as well as for different compositions x in $GaAs_{1-x}P_x$. These data clearly show a smooth trend in both the absolute value of the thermal emission rate and the corresponding energy with variation in composition.

The photoionization cross section, $\sigma_n^o(h\nu)$, for optically promoting an electron from the deep *EL*2 donor level to the conduction band in GaAs is also well known.[17] Figure 2 shows spectra of $\sigma_n^o(h\nu)$ measured using the initial part of the photocapacitance transients for different alloy compositions. In GaAs the $\sigma_n^o(h\nu)$ spectrum starts at roughly half the band gap exhibiting a "kink" around 1.1 eV. With increasing x a smooth trend is observed in both the magnitude of $\sigma_n^o(h\nu)$ and the threshold and shape of the spectra. These data further suggest that the deep centers studied in the alloys are related to *EL*2 in GaAs.

The most peculiar property observed for GaAs:*EL*2 is the photocapacitance quenching effect and the appearance of a metastable state.[9,18–20] The photocapacitance quenching effect is shown in Fig. 3 for $x=0.20$. This behavior is, in principle, identical to that obtained for *EL*2 in GaAs. These results indeed confirm that the same type of transformation of the "normal" deep state to a metastable state occurs in the alloys. Although this effect, for yet unknown reasons, seems to disappear for $x>0.3$,[9] data like those in Fig. 3 strongly suggest that *EL*2-like states also exist in the alloys. Therefore, from the data on thermal emission rates, optical photoionization cross sections, and photocapacitance quenching properties we conclude that the deep levels studied in the $GaAs_{1-x}P_x$ alloy system are indeed related to the *EL*2 defect in GaAs.

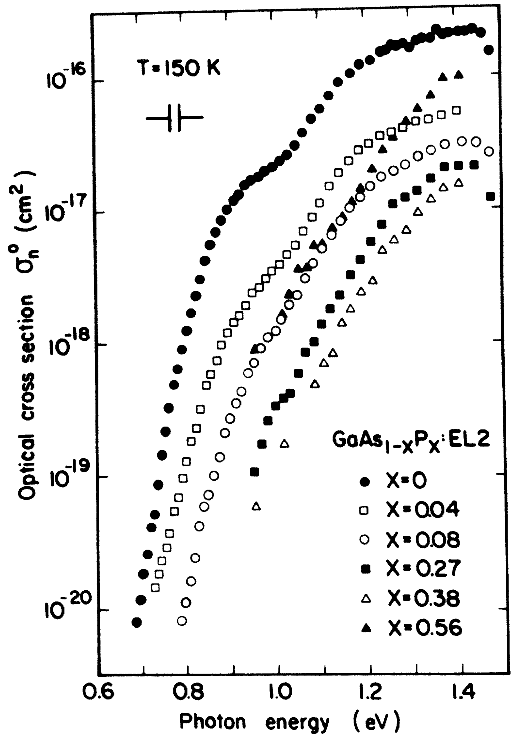

FIG. 2. Absolute values of optical cross sections σ_n^o plotted versus photon energy for the *EL*2 level in GaAs and in different $GaAs_{1-x}P_x$ alloys.

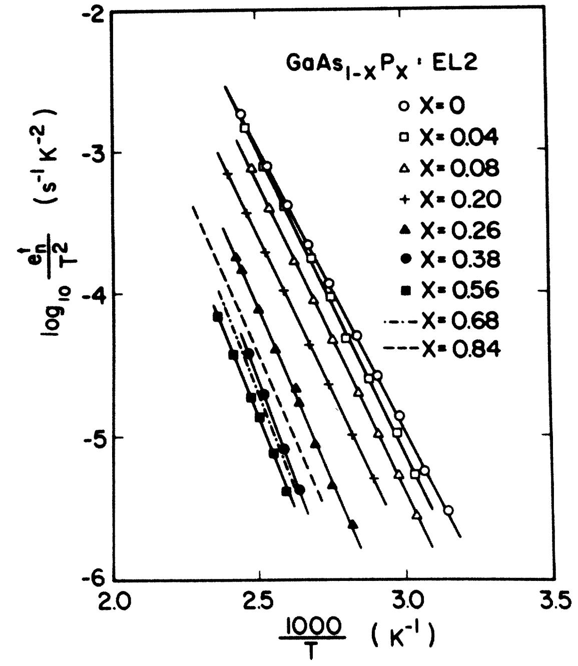

FIG. 1. Thermal emission rates (T^2 corrected) versus inverse temperature for the *EL*2 level in GaAs and in different $GaAs_{1-x}P_x$ alloys.

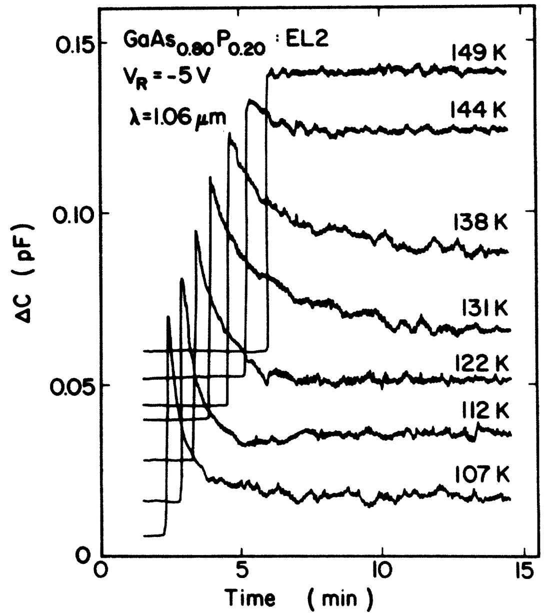

FIG. 3. Photocapacitance quenching effect, typical for *EL*2 in GaAs, as observed for the corresponding *EL*2 defect in $GaAs_{0.80}P_{0.20}$ (from Ref. 9).

TABLE I. Thermal, optical, and deep-level broadening properties of the *EL*2 level in $\mathrm{GaAs}_{1-x}\mathrm{P}_x$. E_A^t is the thermal activation energy from Fig. 1, FWHM is the full width at half maximum of the alloy broadening of the deep levels, κ is the correction factor by which the apparent DLTS concentration has to be multiplied in order to get the correct concentration N_T. E_{th}^o is the optical threshold energy deduced relative to the value 0.75 eV in GaAs as described in Sec. III C.

x in $\mathrm{GaAs}_{1-x}\mathrm{P}_x$	E_A^t (eV)	FWHM (meV)	κ	N_T (10^{13} cm^{-3})	E_{th}^o (eV)
0	0.79	0	1	14	0.75
0.04	0.83	28	1.06	12	0.77
0.08	0.86	31	1.07	8	0.83
0.20	0.88	42	1.11	6	
0.26	0.92	78	1.31	6	0.96
0.38	1.07	113	1.64	8	1.06
0.56	1.00	131	1.73	14	1.17
0.68	1.07			(≈9)	
0.84	0.99	47	1.13	1	

B. Thermal emission data

Our thermal emission data for *EL*2-related defects show a smooth trend for the $\mathrm{GaAs}_{1-x}\mathrm{P}_x$ alloy system (Fig. 1). However, with increasing x the individual DLTS peaks become broadened (solid lines in Fig. 4). Using a model and a fitting procedure for alloy-broadened deep levels (previously published[13]), computer fits (symbols in Fig. 4) were made to our experimental curves. Thermal activation energies (E_A^t), corrected deep-level concentrations and full widths at half maximum (FWHM's) of the broadened impurity levels obtained from these fits are collected in Table I (for details of this fitting procedure see Ref. 13). The FWHM's of the broadened impurity levels are also plotted in Fig. 5 as a function of alloy composition. As expected, the broadening is largest close to $x = 0.5$, where the alloying is most pronounced.

A model has been developed[21] for alloy-broadened defect levels, where it was shown that the energy width of a defect can be used to estimate an effective sampling radius of the defect. This model, applied to the data in Fig. 5 and in Table I, suggests that the *EL*2 wave function is strongly localized with an effective radius of 5—10 Å. This makes *EL*2, not only with regard to the binding energy, a truly "deep level." To compare the estimated ex-

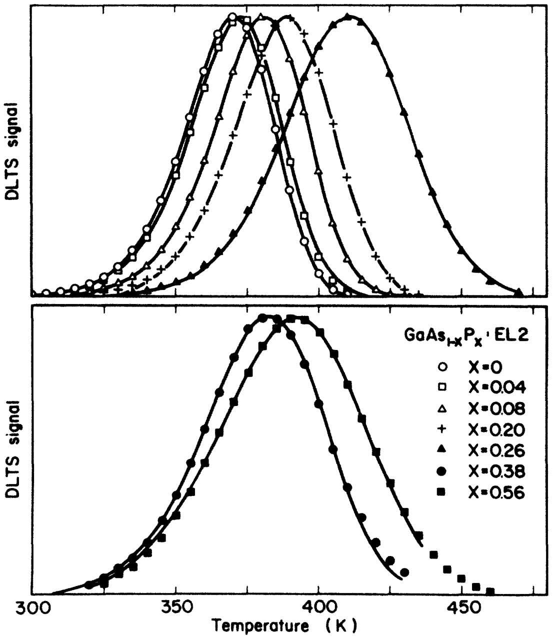

FIG. 4. Experimental DLTS spectra (solid lines) recorded for various alloy compositions x in the $\mathrm{GaAs}_{1-x}\mathrm{P}_x$:*EL*2 system. The rate window is 24 s^{-1} in the upper figure and 1.2 s^{-1} in the lower figure. Also shown are theoretical fits (symbols) to experimental spectra yielding values of S and κ, where S is a measure of the deep level broadening and κ is a correction factor for concentration determination (see Table I).

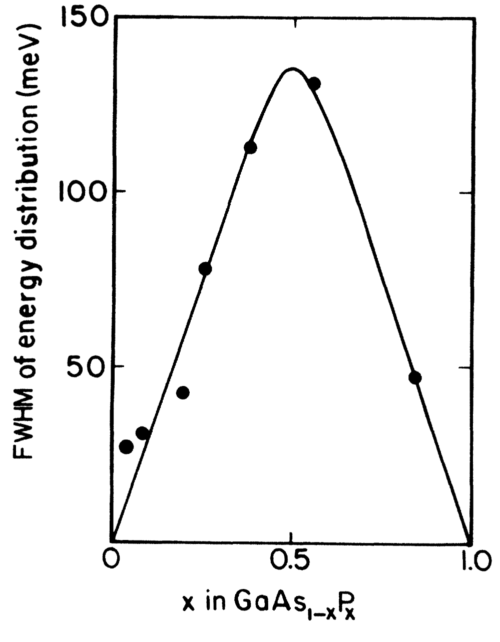

FIG. 5. Experimentally determined energy level distribution (FWHM) of *EL*2 as a function of x in $\mathrm{GaAs}_{1-x}\mathrm{P}_x$. The solid line is only to guide the eye.

tent of the wave function one may take the simple model of a δ-function potential with its corresponding wave function[22]

$$\Psi(r)=\sqrt{\alpha/2\pi}e^{-\alpha r}/r \text{ with } \alpha^2=2m^*E_i/h^2 .$$

If, for simplicity, the electron effective mass is used for m^*, the radius (r') within which 80% of the charge density of the bound electron is located becomes $r'\approx 7$ Å. In spite of the crudeness of the δ-function potential model and of the evaluation of the energy-level broadening, the agreement between the two models is quite encouraging. The localized character of the *EL*2 state is supported by the strong phonon coupling observed in optical and thermal excitations[1] which, in a Fröhlich picture,[23] suggests that excitations of *EL*2 are accompanied by significant changes in the local electrostatic interaction. A more detailed analysis and interpretation of the variation in the electron energy FWHM with alloy composition is, however, beyond the scope of this paper.

C. Photoionization cross sections

It is believed that the shape of the $\sigma_n^o(h\nu)$ spectrum of *EL*2 in GaAs (Fig. 2) is due to a superposition of contributions from transitions to different conduction bands.[17] If this interpretation is correct, the expected variation in the spectral distribution of the photoionization cross section for *EL*2 in the $\mathrm{GaAs}_{1-x}\mathrm{P}_x$ alloys can be anticipated since the variation in the band structure with x is known with reasonable accuracy. In order to determine optical threshold energies of *EL*2 for different alloy compositions x, it was therefore assumed that the three dominant components of the experimental $\sigma_n^o(h\nu)$ spectrum of GaAs: *EL*2 are generated by transitions from the *EL*2 level to the lowest Γ, *L*, and *X* parts of the GaAs conduction band. For each value of x studied, the *L* and *X* components were shifted relative to the fixed Γ component, in accordance with the variation in the conduction-band minima, and added. Comparing these generated spectra with measured $\sigma_n^o(h\nu,x)$ spectra it was observed that the experimental spectra were broadened for large values of x, probably due to random variations in the alloying components. However, using the generated spectra, and the deduced distribution of the alloy-broadened impurity levels from Table I, the solid lines in Fig. 6 were generated by simple convolution of the shifted theoretical spectra and the Gaussian line shapes for the impurity distribution. The optical threshold energies for the *EL*2 levels in $\mathrm{GaAs}_{1-x}\mathrm{P}_x$ were obtained by measuring how much the generated spectra had to be shifted (along the $h\nu$ axis) from the GaAs:*EL*2 Γ value, in order to fit the experimental data. The optical threshold energies for *EL*2 in the alloys are therefore obtained relative to the optical threshold energy in GaAs. The optical threshold energies (E_{th}^o) obtained in this way are summarized in Table I.

The fitting of generated σ_n^o spectra to experimental results of $\sigma_n^o(h\nu)$ (Fig. 6) is based on the assumption that the shape of the spectra is determined only by transitions to different conduction band minima. In a recent paper[24] it was argued that the kink at ≈ 1.1 eV in GaAs originates mainly from an internal transition within the *EL*2 defect. It has, however, been reported previously that the energy and the spectral shape of this internal transition is independent of composition.[9] Since the thermal data presented below (Fig. 7) show that the ground state of *EL*2 is more or less fixed relative to the *L* band (see Sec. III D), this alternative would not have a strong effect on the fitting procedure.

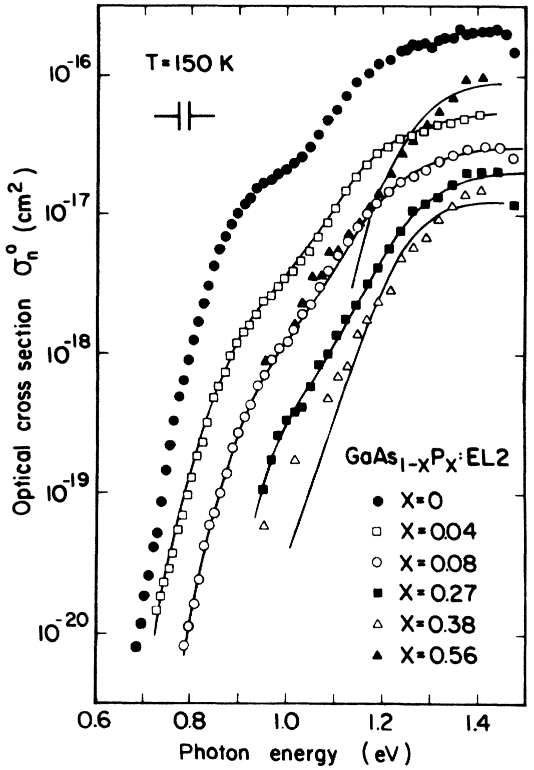

FIG. 6. Optical cross sections, σ_n^o, for *EL*2 in $\mathrm{GaAs}_{1-x}\mathrm{P}_x$ fitted with the model (solid line) described in Sec. III C.

D. Trends in ground-state properties of $\mathrm{GaAs}_{1-x}\mathrm{P}_x$:*EL*2

The thermal activation energies presented in Sec. III B and the optical threshold energies deduced in Sec. III C (summarized in Table I) are plotted in Fig. 7 relative to the $\mathrm{GaAs}_{1-x}\mathrm{P}_x$ band structure. Figure 7 shows that, within experimental error, the thermal and optical data suggest a continuous and smooth variation with x, and that the energy distance of the *EL*2 ground state ($EL2^g$) from the lower edge of the *L* band is almost constant. Hence, the procedures used for the evaluation of thermal and optical energies are justified by the fact that thermal and optical data gave similar results. It is therefore tempting to extrapolate the different energy values obtained for different values of x to $x=1.0$ in order to compare them with thermal and optical data of identified defects in GaP. We have in Fig. 7 included data for $x=1.0$ for the oxygen ($\mathrm{O_P}$) level,[3,25] the phosphorous antisite $\mathrm{P_{Ga}}$ defect[26-29] (sometimes denoted $\mathrm{PP_4}$), the $\mathrm{PP_3}Y_\mathrm{P}$ defect[26-29] (a $\mathrm{P_{Ga}}$ defect surrounded by three regular phosphorous atoms and one unknown atom Y on the P sublattice) and the nickel d^9 ($\mathrm{Ni_{Ga}}^+$) level.[30] All these

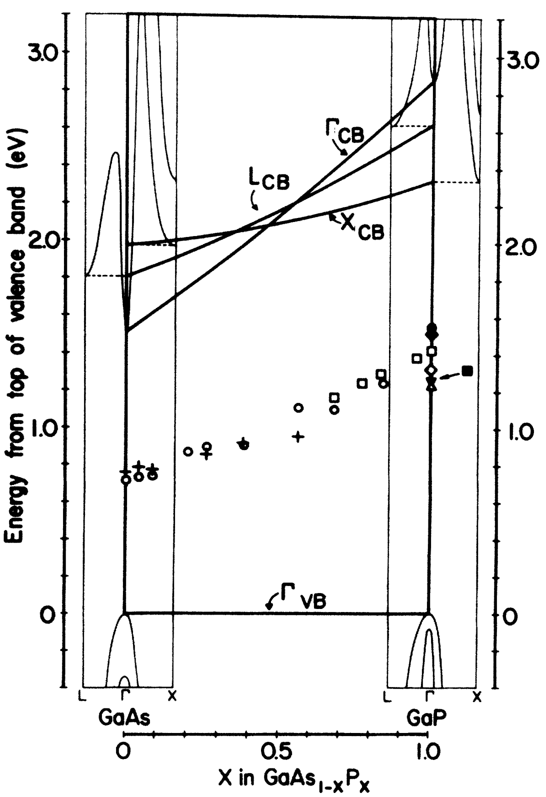

FIG. 7. Thermal activation energies (○) and optical threshold energies (+) plotted relative to the $GaAs_{1-x}P_x$ band structure. Also given are thermal (■) and optical (□) data for oxygen (Refs. 3 and 25), optical data (△,▽) for P_{Ga} (PP_4) (Refs. 26–29), optical data (●) for P_{Ga} (PP_3Y_P) (Ref. 29), optical data (♦) for Ni (Ref. 30), and thermal data for the *D*5 level (◇) (Ref. 36) in GaP. The optical oxygen data (□) from Ref. 31 for different x in $GaAs_{1-x}P_x$ are also included. CB is the conduction band, VB the valence band.

levels fall within the relatively narrow range of energies obtained by extrapolating our *EL*2 data in $GaAs_{1-x}P_x$ to GaP. For historical reasons we start with the data for GaP:O (Ref. 3) and have therefore also plotted optical energies obtained from data for oxygen-implanted $GaAs_{1-x}P_x$ from $x = 1.0$–0.6 (Ref. 31) in Fig. 7. Although the agreement between the binding energies of *EL*2 and of oxygen in $GaAs_{1-x}P_x$ is quite good, there are strong arguments against the connection between the two cases. One such argument is that the incorporation of *EL*2 varies as the square root of the AsH_3 partial pressure during epitaxial growth, hence suggesting a relation between the formation mechanism of *EL*2 and vacant group-III sites (V_{Ga}).[4] Oxygen, on the contrary, is (in GaP) known to occupy a group-V site.[3] Furthermore, Huber *et al.*[32] have measured oxygen concentrations considerably lower than that of *EL*2, and Wagner *et al.*[33] found that the concentration of *EL*2 was not affected by the presence of, for oxygen, highly reactive trimethylaluminium during growth.

Another experimental result opposing a connection between the trends of oxygen and *EL*2 in the $GaAs_{1-x}P_x$ alloy is found from a plot of the alloy dependence of absolute numbers of thermal emission rates, e_n^t, taken at one fixed temperature. Values of e_n^t obtained at $T = 400$ K decrease in the direct-gap region when x increases from $x = 0$ (i.e., GaAs) as shown in Fig. 8. This is to be expected from the data in Fig. 7, where thermal activation energies as well as optical threshold energies are shown to increase in this alloy region. Since the energetic position of the *EL*2 level varies roughly linearly with x, with a slope similar to that of the L minimum and, hence, between those of the Γ and X minima, a maximum of the binding energy is expected for $x \approx 0.48$, i.e., the composition where the Γ and X conduction-band minima intersect. A corresponding change in the slope is clearly seen in the thermal emission data $e_n^t(T = 400\text{ K})$ versus x around $x = 0.5$ (Fig. 8). Obviously, the energetic separation between the *EL*2 level and the X minimum decreases for $x > 0.5$ (see Fig. 7) which is directly reflected in the increasing magnitude of thermal emission data in Fig. 8. Therefore, in addition to the optical and thermal energies in Fig. 7, we have a third tracer to bring to $x = 1.0$. i.e., GaP. On the thermal emission axis corresponding to $x = 1.0$, e_n^t data from the literature are indicated for different defects. Here it is seen that the *EL*2 data extrapolate to emission rates differing from those of GaP:O by several orders of magnitude.

The other GaP defects in this energy range taken into consideration here are all possible candidates for *EL*2 judged from the stoichiometric conditions under which the P_{Ga}, Ni_{Ga}, and *EL*2 defects occur. It is interesting to note that in GaAs, *EL*2 has been connected with the arsenic antisite (As_{Ga}) defect.[8] However, it is not obvious that an energy level from an isolated As_{Ga} defect could be continuously transformed into an energy level for the isolated P_{Ga} defect. As a speculation, if As_{Ga} is part of the

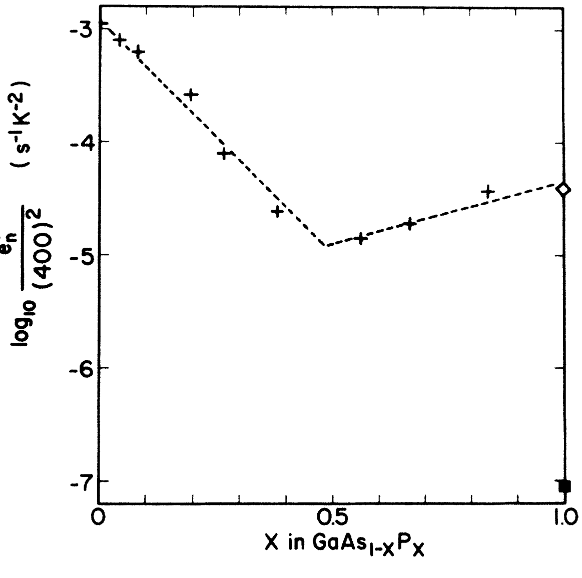

FIG. 8. The logarithm of the (T^2 corrected) thermal emission rate for the *EL*2 defect at $T = 400$ K plotted versus x in $GaAs_{1-x}P_x$ (+). Also included are emission rates for oxygen (■) (Ref. 25) and the *D*5 level (◇) (Ref. 36) in GaP.

*EL*2 defect, this might mean that the energy level is actually determined by a second constituent of an antisite-containing complex. It is interesting to note that both $\mathrm{As_{Ga}}$ (Ref. 34) and $\mathrm{P_{Ga}}$ (Refs. 26 and 29) have been observed in different complexes which may support this idea.

Ni has been reported to be a persistent contaminant in VPE-grown GaP materials.[30,35] In GaAs the experimental results seem to be unclear. To the best of our knowledge no reports of Ni concentrations have been published. It seems, however, unlikely, with the high concentrations of *EL*2 found in semi-insulating GaAs, that such high concentrations of Ni should have avoided detection.

When GaP is grown with stoichiometric conditions similar to those used to form *EL*2 in the $\mathrm{GaAs_{1-x}P_x}$ alloy system, the DLTS spectra of the as-grown material become more complicated than for the alloys.[36] At least six deep traps are normally observed, but only two of these unknown levels have reasonable activation energies to be candidates for the *EL*2 level in GaP. However, only one of these levels is consistent with the extrapolation to $x=1.0$, both for the activation energy (see Fig. 7) and for the thermal emission rate at $T=400$ K (see Fig. 8). This level, which is denoted *D*5 in Ref. 36, also increases in concentration with increasing phosphorous partial pressure during growth. We therefore suggest that this level is the corresponding *EL*2 level in GaP. Further investigations on this defect are, however, needed before a definite assignment can be made. It is, for instance, not clear whether or not this is the same energy level that has been reported to be related to the $\mathrm{P_{Ga}}$ defect.

E. Trends in excited state properties of $\mathrm{GaAs_{1-x}P_x}$:*EL*2

The energy level of the ground state of *EL*2 ($EL2^g$) is plotted versus x in Fig. 7. In GaAs the transformation from this ground state to the metastable state ($EL2^*$) takes place via a branching state.[9,24] This branching state has been interpreted as an excited state ($EL2^e$) of the neutral *EL*2. Since it was previously observed that the spectral distribution of this internal excitation is not affected by alloying ($x<0.3$),[9] it is possible to plot both the ground state and the excited state in the band diagram for the $\mathrm{GaAs_{1-x}P_x}$ system (Fig. 9). An obvious observation is the fact that the excited state seems to emerge out of the conduction band at $x \approx 0.3$, i.e., the x value where the metastable properties of *EL*2 have been reported to disappear.[9] If this observation is assumed to be relevant, two qualitative explanations for the disappearance of the metastable properties for $x>0.3$ can be suggested. First, the excited state might actually disappear when it merges out of the conduction band. It is, however, hard to construct a mechanism for such a disappearance of an electronic state. Second, it may be necessary for the excited state to be degenerate with the conduction-band states in order for it to populate or transform to the metastable state. In such a case the transition probability (i.e., the matrix element for transformation of the excited $EL2^e$ state to the metastable state $EL2^*$) is negligible when the excited state is nondegenerate, but has a finite value when degenerate with the continuum of conduction-band states. A possible reason for such changes in the transition probability could be changes in the $EL2^e$ wave function when it becomes degenerate with the conduction band. Such changes in a defect wave function have been reported for N in $\mathrm{GaAs_{1-x}P_x}$.[37] The latter mechanism suggests that the excited state is present in the band gap in $\mathrm{GaAs_{1-x}P_x}$ when $x>0.3$, and should in principle be observed in absorption measurements. Unfortunately, the material available is too thin (a few micrometers) for absorption measurements. The excited state could, however, be observed if it is optically populated followed by thermal excitation to the conduction band. Therefore, it is interesting to observe in Fig. 7 that the photoionization cross sections determined from photocapacitance measurements show clear deviations from the calculated curves on the low-energy side for $x>0.3$. This could in fact be caused by absorption to the $EL2^e$ state followed by thermal emission to the conduction band, a process which is expected to be quite efficient at the temperature of the measurements $T=150$ K. Even though the reason and the detailed explanation for the disappearance of the metastable state for $x>0.3$ still has to be considered as unknown, we feel that any valid model for the *EL*2 defect should be able to explain these results.

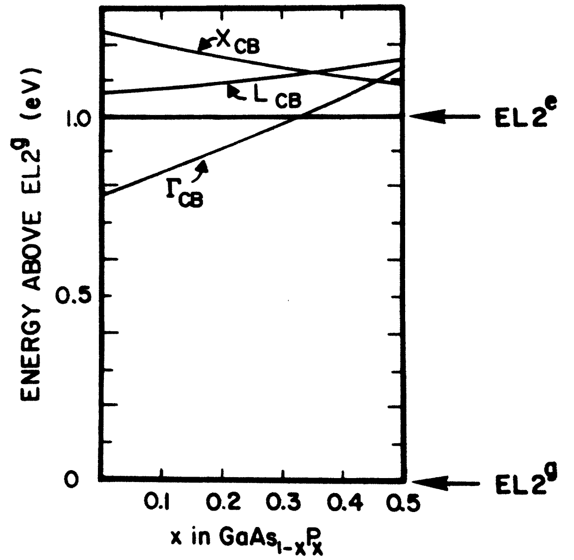

FIG. 9. The trend in the positions of the excited ($EL2^e$) states of *EL*2 plotted relative to the varying conduction band (CB) structure of $\mathrm{GaAs_{1-x}P_x}$, with the ground ($EL2^g$) state used as the horizontal reference level.

IV. CONCLUSIONS

Data have been presented which show the existence of an *EL*2-related defect in $\mathrm{GaAs_{1-x}P_x}$. From optical and thermal measurements properties of the ground state of *EL*2 are traced in the alloy system. Extrapolation of the alloy-dependent properties to GaP enables us to strongly reduce the number of possible candidates for an *EL*2-related defect in GaP. Combining ground-state properties with previously published properties of excited states of *EL*2 in the alloy system suggests that population of the metastable *EL*2 state requires that the excited state be degenerate with the conduction band.

ACKNOWLEDGMENT

The authors are pleased to acknowledge H. G. Grimmeiss for critical reading of the manuscript.

---

[1] For a review see G. M. Martin and S. Makram-Ebeid, in *Deep Centers in Semiconductors,* edited by S. T. Pantelides (Gordon and Breach, New York, 1985), p. 399.

[2] A. G. Milnes, *Deep Impurities in Semiconductors* (Wiley, New York, 1973), p. 59.

[3] P. J. Dean, C. H. Henry, and C. J. Frosch, Phys. Rev. **168**, 812 (1968).

[4] L. Samuelson, P. Omling, H. Titze, and H. G. Grimmeiss, J. Cryst. Growth **55**, 164 (1981).

[5] J. Lagowski, H. G. Gatos, J. M. Parsey, K. Wada, M. Kaminska, and W. Walukiewicz, Appl. Phys. Lett. **40**, 243 (1982).

[6] D. E. Holmes, K. R. Elliot, R. T. Chen, and C. G. Kirkpatrik, in *Semi-Insulating III-V Materials,* edited by S. Makram-Ebeid and B. Tuck (Shiva, Nantwich, 1982), p. 19.

[7] E. R. Weber, H. Ennen, U. Kaufmann, I. Windscheif, J. Schneider, and T. Wosinski, J. Appl. Phys. **53**, 6140 (1982).

[8] For a review see E. R. Weber and P. Omling, in *Festkörperprobleme, Advances in Solid State Physics,* edited by P. Grosse (Vieweg, Braunschweig, 1985), Vol. XXV, p. 622.

[9] P. Omling, L. Samuelson, and H. G. Grimmeiss, Phys. Rev. B **29**, 4534 (1984).

[10] L. Samuelson, P. Omling, H. Titze, and H. G. Grimmeiss, J. Phys. (Paris) Colloq. **12**, C5-323 (1982).

[11] P. Omling, L. Samuelson, H. Titze, and H. G. Grimmeiss, Nuovo Cimento **2**, 1742 (1982).

[12] D. V. Lang, J. Appl. Phys. **45**, 3014 (1974).

[13] P. Omling, L. Samuelson, and H. G. Grimmeiss, J. Appl. Phys. **54**, 5117 (1983).

[14] H. G. Grimmeiss and C. Ovrén, J. Phys. E **14**, 1032 (1981).

[15] M. O. Watanabe, A. Tanaka, T. Udagawa, T. Nakanisi, and Y. Zohta, Jpn. J. Appl. Phys. **22**, 923 (1983).

[16] J. Lagowski, D. G. Lin, T. Aoyama, and H. C. Gatos, Appl. Phys. Lett. **44**, 336 (1984).

[17] A. Chantre, G. Vincent, and D. Bois, Phys. Rev. B **23**, 5335 (1981).

[18] G. Vincent and D. Bois, Solid State Commun. **27**, 431 (1978).

[19] A. Mitonneau and A. Mircea, Solid State Commun. **30**, 157 (1979).

[20] G. Vincent, D. Bois, and A. Chantre, J. Appl. Phys. **53**, 3643 (1982).

[21] L. Samuelson, J. Electron. Mater. **14A**, 101 (1985).

[22] M. Jaros, J. Phys. C **4**, 1162 (1971).

[23] Y. Toyozawa, in *Dynamical Processes in Solid State Optics,* edited by R. Kubo and H. Kamimura (Benjamin, New York, 1967), p. 90.

[24] M. Kaminska, M. Skowronski, J. Lagowski, J. M. Parsey, and H. C. Gatos, Appl. Phys. Lett. **43**, 302 (1983).

[25] C. H. Henry and D. V. Lang, Phys. Rev. B **15**, 989 (1977).

[26] K. P. O'Donnell, K. M. Lee, and G. D. Watkins, Solid State Commun. **44**, 1015 (1982).

[27] U. Kaufmann, J. Schneider, R. Wörner, T. A. Kennedy, and N. D. Wilsey, J. Phys. C **14**, L951 (1981).

[28] N. Killoran, B. C. Cavenett, M. Godlewski, T. A. Kennedy, and N. D. Wilsey, J. Phys. C **15**, L723 (1982).

[29] B. K. Meyer, Th. Hangleiter, J.-M. Spaeth, G. Stranch, T. Zell, A. Winnacker, and R. H. Bartram, J. Phys. C **18**, 1503 (1985).

[30] X.-Z. Yang, L. Samuelson, and H. G. Grimmeiss, J. Phys. C **17**, 6521 (1984).

[31] D. J. Wolford, S. Modesti, and B. G. Streetman, *Proceedings of the 10th International Symposium on GaAs and Related Compounds,* Inst. Phys. Conf. Ser. No. 65, edited by G. E. Shillman (IOP, Bristol, 1982), p. 477.

[32] A. M. Huber, N. T. Linh, M. Valladon, J. L. Debrun, G. M. Martin, A. Mitonneau, and A. Mircea, J. Appl. Phys. **50**, 4022 (1979).

[33] E. E. Wagner, D. E. Mars, G. Hom, and G. B. Stringfellow, J. Appl. Phys. **51**, 5434 (1980).

[34] For a review see J. M. Spaeth and B. K. Meyer, *Festkörperprobleme, Advances in Solid State Physics,* edited by P. Grosse (Vieweg, Braunschweig, 1985), Vol. XXV, p. 613.

[35] P. J. Dean, A. M. White, B. Hamilton, A. R. Peaker, and R. M. Gibb, J. Phys. D **10**, 2524 (1977).

[36] X.-Z. Yang, L. Samuelson, H. G. Grimmeiss, and P. Omling (unpublished).

[37] D. J. Wolford, B. G. Streetman, Shui Lai, and M. V. Klein, Solid State Commun. **32**, 51 (1979).